ANOMALOUS X-RAY SCATTERING FROM TERBIUM-LABELED PARVALBUMIN IN SOLUTION

RICHARD C. MIAKE-LYE, S. DONIACH, AND KEITH O. HODGSON
Departments of Applied Physics and Chemistry, Stanford University, Stanford, California 94305

ABSTRACT We have used anomalous small-angle x-ray scattering as a structural probe for solutions of rabbit parvalbumin labeled with terbium. This technique makes use of the large changes in the terbium scattering factor that occur when the x-ray energy is tuned around an L_3 absorption edge of this heavy-atom label. These changes in scattering result in changes in the small-angle scattering curve of the labeled protein as a whole, which can then be analyzed to derive structural information concerning the distribution of labels in the protein. Based on a Gaussian model for the protein electron density, the mean distance from the terbiums to the protein center of mass is determined to be 13.2 Å and is consistent with crystallographic results. Our results demonstrate the usefulness of terbium as an anomalous scattering label and provide criteria to help establish anomalous scattering as a reliable structural technique for proteins in solution.

INTRODUCTION

The availability of high intensity, continuously tuneable x-ray beams from synchrotron radiation sources has created new possibilities for the use of small-angle x-ray scattering in structural studies of proteins in solution. Conventional small-angle x-ray scattering is used to measure general size and shape parameters of a molecule in solution (1). By tuning the x-ray energy through an absorption edge of a heavy atom bound in the molecule, additional structural information can be obtained. By making use of the anomalous scattering contribution of the heavy atom to the total scattering curve, specific structural parameters can be determined (2–4). In particular, using a model for the protein electron density, one can measure the distance of the heavy atom from the center of mass of the molecule. In the case of a molecule with two or more identical heavy atoms, the distance between the heavy atoms may also be determined; this determination is model independent.

In this paper we report a feasibility study on the use of anomalous x-ray scattering to obtain structural information about the calcium binding sites in parvalbumin in which the two bound Ca^{2+} ions have been replaced with Tb^{3+} ions. We show that the mean distance from the terbium ions to the protein center of mass is readily measured. Further, the direct observation of the terbium-terbium interference term in the scattering profile should be possible with the x-ray flux available from contemporary wiggler-magnet synchrotron radiation sources. Measurements of this type will enable the observation of conformational changes in noncrystalline protein samples caused by changes in the chemical or physical environment of the protein.

Anomalous scattering induces changes in the x-ray scattering from a given atom as the photon energy is tuned through an inner-shell absorption edge. These changes occur in both the amplitude and the phase of the scattered x-ray wave. By using a heavy-atom label that has a pronounced anomalous scattering effect and whose inner-shell ionization threshold (absorption edge) is far from those of the bulk of the molecule, those terms in the scattering curves involving the label can be selectively altered. By measuring scattering curves at several x-ray energies and computing the differences between them, these terms can be extracted and analyzed to determine the label's relative position in the molecule.

Recent work by Stuhrmann and Notbohm (3, 4) has made use of iron as an anomalous scattering label in studies of hemoglobin and ferritin. While the native iron was used to advantage in these cases, the workers note that the size of the anomalous scattering change in iron limits both the amount of information (number of terms) extracted and the concentration of protein used in an experiment.

Due to details of atomic structure involving empty atomic d-levels (5),[1] the lanthanides and some of the heavy transition metals have particularly strong and sharp absorption edge features at their L_3 edges ($^2P_{3/2}$ ionization threshold, see Fig. 1). For these elements, changes in the scattering factor of ~20 electrons are observed (2)[2] near the peak in absorption at the edge (the "white line") vs. ~5

[1]Kutzler, F. W., D. K. Misemer, S. Doniach, and K. O. Hodgson. 1982. Theory of white lines in the x-ray absorption spectra of lanthanide complexes. Submitted to *Chem. Phys. Lett.* 92:626–630.

[2]Templeton, L. K., D. H. Templeton, R. P. Phizackerly, and K. O. Hodgson. 1982. L_3-edge anomalous scattering by gadolinium and samarium measured at high resolution with synchrotron radiation. *Acta Cryst.* A38:74–78.

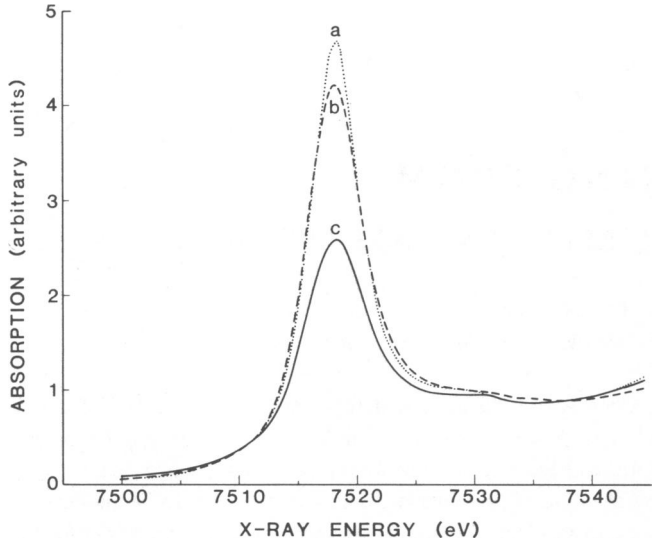

FIGURE 1 X-ray absorption spectra in a region including the terbium L_3 absorption edge. The spectra were taken at SSRL beam line I-5 using a standard transmission EXAFS setup (15) and Si 220 monochromator crystals. (*a*) 60mM $TbCl_3$ buffered to pH 5.5 with 100 mM MES. (*b*) as *a* with 20 mM EDTA (ethelenediaminetetraacetic acid). (*c*) as *a* with 30 mM rabbit parvalbumin. Note that the position of the edge does not change, but the height of the absorption peak (white line) depends on the coordination environment.

electrons for iron (3, 4). Because the energies of their L_3 edges are easily reached with a synchrotron radiation source, these elements make ideal anomalous scattering labels. The fact that many of the lanthanides can replace calcium in biological systems makes them particularly attractive for use in structural studies of calcium binding proteins.

The calcium ion plays an important role in biological regulation and yet this ion is not observable by most spectroscopic methods. This has led to the development of lanthanide substitution as a probe to study the structure and function of calcium binding proteins (6–8). Parvalbumin, which binds two calcium ions, was chosen for our feasibility studies because it is a small protein (11,500 daltons), and its refined crystal structure (9, 10) is available for comparison with our results.

The work reported here establishes the magnitude of the changes (5–7%) in the parvalbumin scattering curve as the x-rays are tuned through the L_3 absorption edge of the terbium label, and demonstrates that the structural information derived corresponds well with theoretical scattering curves calculated using coordinates derived from the crystal structure. Although the statistical accuracy achieved so far (0.25–0.5%) and problems in absorption corrections do not allow the extraction of the terbium-terbium interference term, we have been able to establish the instrumental accuracy and experimental conditions needed to make this measurement possible. The terbium-to-protein center of mass distance that we report here, especially when used in conjunction with the terbium-terbium distance that we plan to determine from measurements using improved experimental equipment, can provide a specific measure of changes in conformation of proteins in solution.

MATERIALS AND METHODS

Parvalbumin from rabbit muscle was obtained from Sigma Chemical Co. (Saint Louis, MO). Parvalbumin from carp was prepared by the method of Pechére (11). (We are grateful to Dr. R. Kretsinger, University of Virginia, for sending us a small sample of carp parvalbumin to help us characterize our preparation.) Terbium chloride was obtained from Alfa (Danvers, MA). Terbium binding to the protein was verified by fluorescence titration (12), buffered to pH 5.5 with MES (2-[*n*-morpholino]ethanesulfonic acid) at a 5.0 μM protein concentration. A protein phenylalanine residue was excited at 259 nm and, after a fluoresence energy transfer, terbium fluorescence was monitored in the range 440–500 nm. Simple two-equivalent binding was observed. The scattering experiments were performed at much higher protein concentrations (30 mM with 2.25 equivalents of Tb added in 100 mM MES at pH 5.5).

The scattering experiments were performed at the Stanford Synchrotron Radiation Laboratory (SSRL) using a focused bending-magnet x-ray beam line (II-2). A platinum-plated focusing mirror, accepting 5.6 mrad from the source bending magnet, situated halfway between the electron orbit and the x-ray scattering camera (total separation 22.7 m) serves to both focus the beam and to filter out higher harmonic radiation. A two-crystal monochromator using the silicon 220 reflection for energy selection was just upstream of the camera.

X-ray Scattering Camera

The camera consists of a collimator/ionization chamber, a sample holder, an evacuated scattering path, and a linear position-sensitive detector. An important feature of the camera is the use of a fluorescent screen and photodiode in the beam stop, just before the detector, to measure the x-ray flux passing through the sample. The ionization chamber in the collimator measures the x-ray flux before the sample. The detector, a 10-cm position-sensitive proportional counter, measures the scattered photons over a range of angles about the direct beam's path. The detector's signal, position encoded by the RC-encoding method (13, 14), is accumulated on a multichannel analyzer (MCA), and has a practical position resolution of ~1 mm including the effects of the beam shape. The two flux measurements, the accumulated scattering curve, and the x-ray energy selected by the monochromator are transferred to the dedicated beam-line computer (Digital Equipment Corp., Maynard, MA, DEC 11/34) and are stored for later analysis. A more complete description of this apparatus will appear elsewhere.

Data Collection

Scattering curves were collected at three energies about the L_3 edge of terbium (below the edge, 7,465 eV; the edge infection point, 7,515 eV; the "white line" absorption maximum, 7,518 eV). Count rates in the neighborhood of 10,000 cps were obtained for storage ring conditions of 60 mA and 3.0 GeV circulating electron energy. The illuminated sample size was typically 1 mm by 1 mm by 1 mm; the sample-to-detector distance was 20 cm; and the detector was placed with 5 cm active length on either side of the direct beam. The measured range of scattering vector, $s = (2\sin\theta)/\lambda$, was ~0.015–0.15 $Å^{-1}$.

The dedicated beam-line computer coordinated the data collection and monochromator tuning. For improved reliability and as a monitor of sample and equipment stability, scattering curves were collected cyclically for the three energies and the cycle was repeated. Five million counts under the integrated curve, including background counts, were collected for each energy in the cycle. Each curve took less than ~20 min to collect (with ~10^8 photons/s incident on the sample) and 14 cycles were accumulated. This allowed us to achieve counting statistics of 0.25 to

0.5% noise over most of the curve, in agreement with the observed noise level.

The lower count-rate at higher angles was partially compensated for by placing a mask in front of the detector. The mask had an opening that was widest at the ends of the detector and decreased in width linearly toward the center where the beam stop was placed. The changes this mask produced in the scattering curves (which were corrected for in subsequent analysis) decreased the statistical noise at larger angles, by a factor of ~3.

The accumulated scattering curves were corrected to give scattered intensity as a function of scattering vector on a set of equally spaced points, taking into account camera geometry and x-ray energy. The large anomalous scattering effects are inevitably linked to correspondingly large absorption and fluorescence, and these latter effects must be carefully accounted for to be able to correctly scale the scattering curves and subtract backgrounds at different x-ray energies. The changes in absorption of the sample were corrected for by scaling the curve by the flux measured in the beam stop detector after the sample. The x-ray fluorescence from the terbium can be approximately calibrated by measuring the scattering from an aqueous solution of $TbCl_3$ at the same energies and using these curves as backgrounds for the protein curves.

Using terbium in aqueous solution as a background is not entirely satisfactory since the anomalous scattering changes observed do depend on the chemical environment of the scatterer. For terbium we have made absorption studies using a conventional x-ray absorption spectrometer (15) with an energy resolution of ~1.5 eV (Fig. 1), and find that the height of the peak at the edge does vary with the coordinated ligands, although the energy of the edge does not change measurably. This problem, compounded by a systematic variation in our flux measurements (attributed to beam motion) and counting statistics limitations, has prevented us thus far from making the accurate absorption corrections needed for the complete analysis of our data (see below).

Anomalous X-ray Scattering

In general, when an x-ray scatters from an atom, the atom behaves as a pointlike scatterer, with a scattering strength proportional to the number of electrons in the atom. This scattering strength is termed the scattering factor and is denoted f. When the x-ray energy approaches an inner-shell absorption edge, however, the scattered x-ray is phase shifted and attenuated (16). Thus the effective strength of the scatterer is no longer proportional to the number of electrons, and the scattering factor must be corrected:

$$f = f_0 + \Delta f' + i\Delta f'' = f'(E) + if''(E), \qquad (1)$$

where f' and f'' are the real and imaginary parts, respectively, of the effective scattering factor, and are functions of the x-ray energy, E. For an anomalous scattering label like terbium, the largest changes (~20 electrons out of 65) occur within 5–10 eV of the absorption edge energy, 7,515 eV, a change of <1% in energy. Because this energy is thousands of eV away from the absorption edges of carbon, nitrogen, oxygen, and sulfur, the scattering factors of these elements are nearly constant and are close to their unperturbed values. Through the use of synchrotron radiation, which has a continuous spectrum and includes this x-ray region for standard operating conditions at SSRL, the scattering from terbium can be selectively and dramatically altered.

For an assemblage of atoms (a molecule), the scattering from all the atoms interferes to produce a scattering curve dependent on the characteristics of the assembly (1, 16). When a few of the atoms are labels, the observed scattering relative to the contrast medium (water, in our case) can be written as a sum of three terms, one not including any contribution from the labels, one where the labels enter linearly, and one made up entirely of the scattering from the labels:

$$I = I_{\text{protein-protein}} + I_{\text{protein-terbium}} + I_{\text{terbium-terbium}}. \qquad (2)$$

Neglecting anomalous corrections to the nonlabeled atoms, which are quite small (<1%) and nearly constant, the energy dependence of the three terms is

$$\begin{aligned} I_{\text{protein-protein}} &\sim \text{constant} \\ I_{\text{protein-terbium}} &\sim f'(E) \\ I_{\text{terbium-terbium}} &\sim [f'(E)]^2 + [f''(E)]^2. \end{aligned} \qquad (3)$$

For a protein labeled with two terbiums, as is parvalbumin, the $I_{\text{terbium-terbium}}$ term is proportional to the particularly simple form $[1 + \sin(2\pi sR)/2\pi sR]$ (2, 16), where R is the distance between the two terbiums. By measuring the total scattering at several x-ray energies and knowing the expected changes in f' and f'' (from absorption measurements and the Kramers-Kronig transform [2]), it is possible in principle to extract this term from the total scattering curve and thus obtain a direct measure of the terbium-terbium distance in the protein when it is in solution without using a model for the protein electron density.

The relative magnitudes of these terms are simply related when they are extrapolated to zero scattering angle where all atoms scatter in phase. Based on parvalbumin's ~1,300 electrons in excess of the solvent level (see below) and two terbium atoms (atomic number 65), the protein-terbium term is 20% of the protein-protein term, and the terbium-terbium term is 1%. The changes that occur in these terms as a result of changing the x-ray energy lead to a change in the protein-terbium term amounting to 5% of the total scattering and a change in the terbium-terbium term of 0.5%. These numbers are based on changes in f' and f'' of -20 and and $+10$ electrons, respectively, at the L_3 absorption edge.

Due to the signal-to-noise ratio and normalization problems described in Data Collection, the terbium-terbium term was too small to be extracted from the data. On the other hand, our experiments show that this term should be measurable, given an order of magnitude increase in counting statistics and x-ray absorption measurements reliable to the same level. The high flux necessary to achieve these statistics in a reasonable time is presently available from wiggler-magnet beam lines at SSRL, although a faster detector using delay-line position encoding (17, 18) would be also be necessary to take advantage of the high count rates.

The other term involving terbium scattering, the protein-terbium cross term, is simple to observe in our experiments. The change in this term as the energy is tuned amounts to 5–7% of the total scattering. This term represents the spherically averaged interference between each terbium

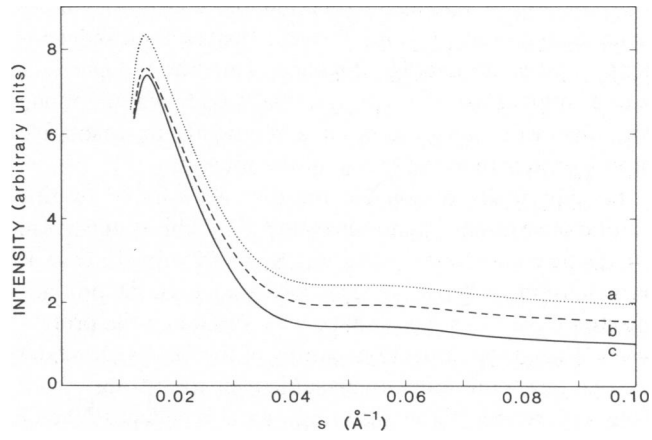

FIGURE 2 Absorption corrected scattering curves for rabbit parvalbumin. The different vertical displacements are due to terbium fluorescence. The different curves were taken at x-ray energies (*a*) 7,518 eV, the absorption peak; (*b*) 7,515 eV, the edge inflection point; and (*c*) 7,465 eV, below the edge. Note that the fluorescence increases as the absorption increases. The change in magnitude of the scattering due to the labeled protein is apparent at smaller s, $s = (2\sin\theta/\lambda$. The beam stop covers the detector for $s < 0.015$ Å^{-1}.

label and the rest of the protein. Through the use of a model for the protein electron density distribution, the simplest case being a Gaussian,[3] this term may be used to extract a terbium to protein center-of-mass distance. In the simplest case, approximating the protein density by a Gaussian electron density distribution; $\rho(r) = \rho \exp(-3r^2/2R_g^2)$, where ρ is the maximum electron density, r is the distance from the center of mass, and R_g is the radius of gyration (density weighted average of r^2); and two terbiums are included as point scatterers at distances R_1 and R_2 from the center of mass, the spherically averaged squared amplitude of the fourier transform becomes

$$I \sim f_{ee}^2 \exp[-(2\pi s R_g)^2/3] + 2f' f_{ee} \exp[-(2\pi s R_g)^2/6] \times \left[\sum_{i=1,2} \sin(2\pi s R_i)/(2\pi s R_i)\right] + I_{\text{terbium-terbium}}. \quad (4)$$

Here f_{ee} is the number of protein electrons in excess of the solvent continuum level, since only relative changes in electron density affect the measurable x-ray scattering. This model can be used to estimate the shape of the scattering curve and the distances R_1 and R_2.

RESULTS AND DISCUSSION

The sums of the fourteen scattering curves for each of the three measured energies are shown in Fig. 2. They have been corrected for camera geometry, x-ray energy, and sample absorption. They have not been corrected for terbium fluorescence, but since this is isotropic it only contributes an additive constant to each curve. The shapes of the curves are fit to a reasonable approximation by a Gaussian in the range $s = 0.02$–0.045 Å^{-1}. This indicated that we should model the protein as a Gaussian electron density distribution to obtain an estimate of R_1 and R_2.

A nonlinear least-squares fitting routine was used to fit the data with the model represented by Eq. 4 over the range $s = 0.02$–0.045 Å^{-1}. The scattering factor terms, f' and f'', can be calculated from the absorption spectrum by using the Kramers-Kronig integral (2). The ratio f'/f_{ee} is not well known (see discussion below) and was floated, as were an overall scaling factor, and the constant fluorescence background. R_1 and R_2 were floated both independently and as an average distance, since the independent fitting resulted in either two essentially equal values or one with that value and the other a physically unreasonable value (greater than the extent of the protein).

The physically reasonable fits that were found by this routine were insensitive to the ratio f'/f_{ee}. This is due to the surprising coincidence among R_g, R_1, and R_2 for the case of parvalbumin. When all three values are equal, the protein-terbium cross term has a shape very similar to the protein term. Within the limits of accuracy of the Gaussian model the two terms are indistinguishable over the fitting range. Thus the shape of the resulting curve is independent of f'/f_{ee} and the fitting routine adjusts the overall scaling factor to compensate for its different values. This means that the shape of the scattering curve should not change with a change in energy (as contrasted with the changes in shape observed in hemoglobin [4]), and this is indeed what was seen. This fact emphasizes the need for accurate sample absorption corrections; we could detect anomalous scattering effects only after we could measure the absorption of the sample with an accuracy of better than a few percent.

From the changes in magnitude of the observed scattering curves we can obtain an estimate of f_{ee}. Based on changes in f' of -20 electrons on going from 7,465 eV (below the edge) to 7,515 eV (edge inflection point) and two terbiums in the molecule, f_{ee} is determined to be 1,330 electrons. To compare this result with the crystallographic structure, we estimated the volume occupied by the protein to be that of an ellipsoid of axes $30 \times 30 \times 36$ Å (9) and assumed the average electron density of the protein to lie in the range 0.41 to 0.43 e/Å^3. (The electron density of water is 0.335 e/Å^3.) These figures yield a theoretical estimate of f_{ee} of 1,300–1,600 electrons. This is consistent with the value of f_{ee} for hemoglobin reported by Stuhrmann (4). When the hemoglobin value of 2,000 is scaled by the respective molecular weights of the proteins, the result is 1,450 electrons for parvalbumin. These estimates indicate that it may be possible to determine the absolute scattering of a protein if f' and f'' of a label are known sufficiently accurately. Using a calibrated scattering standard would remain a more direct approach, however.

The R_g found by the fitting routine, 12.9 Å, is not correctly extrapolated to zero angle and zero concentration (the appropriate data was not collected due to beam-time limitations), but is that of the Gaussian distribution that best fits the curve in the fitting range. As will be shown below by comparison with crystallographic data, however, this is probably a better estimate than it may seem. The best fit to the data, with an rms error of 0.25%, gave the following relevant parameters:

$$R_g = 12.9 \text{ Å } R_1, R_2 = 13.2 \text{ Å}. \quad (5)$$

It appeared that we had indeed chosen a model system that had the coincidental property of having a scattering curve shape essentially independent of the anomalous scattering effect. To substantiate this, we calculated the theoretical scattering curve from the crystal structure of carp parvalbumin (10). Because this structure is based on a protein from a different species than we have used, we have also measured the scattering curve at 7,465 eV for carp parvalbumin. On comparing the scattering from these two proteins, we found that they agree within 1% over the entire range 0.02–0.045 Å^{-1}. This is not surprising since there is a great deal of sequence similarity between these two proteins (of the 109 amino acids in parvalbumin, 24 amino acids are invariant and 17 are highly conserved among several species) and evidence indicates that there are even more structural similarities (19), as is borne out by this comparison. Using the coordinates of the carp

[3]Stuhrmann, H. B. 1970. Interpretation of small-angle scattering functions of dilute solutions and gases. A representation of the structures related to a one-particle scattering function. *Acta Cryst.* A26:297–306.

structure, the corresponding structural parameters are

$$R_g = 12.8 \text{ Å } R_1 = 14.4 \text{ Å } R_2 = 12.7 \text{ Å} \quad (6)$$

(from x-ray crystallographic coordinates of carp parvalbumin). Here R_g is the calculated theoretical radius of gyration based on the actual atomic coordinates, to be distinguished from the fitted result based on the Gaussian model. Note that the average of R_1 and R_2, 13.6 Å, is in reasonable agreement with the result of the curve fit. Fig. 3 shows a comparison between the scattering curve calculated from the x-ray crystallographic coordinates and our measured curve.

Because the calculated radius of gyration is the same as that which we infer from our fit, our use of the Gaussian model in the fitting procedure for parvalbumin is supported. The consistency among the rabbit parvalbumin scattering curve, the carp parvalbumin scattering curve, and the carp parvalbumin crystallography results indicates that, at least on a coarse level (measured by R_g, R_1, R_2, and the overall curve), the structures of these proteins are nearly identical.

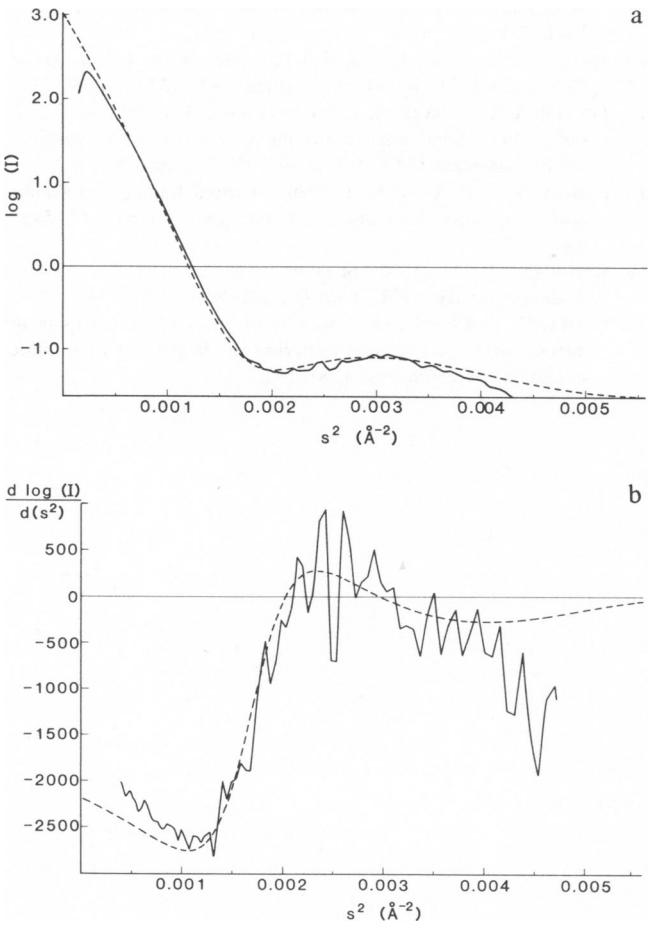

FIGURE 3 (*a*) Guinier plot (log I vs. s^2) for the scattering curve of rabbit parvalbumin (the solid curve, taken at 7,465 eV) and for the theoretical curve calculated from crystallographic coordinates. (*b*) Derivative of *a* showing the discrepancy in slope at small angles. The ordinate is $y = (2\pi R_g)^2/3$. The theoretical curve gives $R_g = 12.8$ Å ($y = 2{,}170$ Å^2); the experimental curve extrapolates to $\sim R_g = 11.8$ Å ($y = 1{,}840$ Å^2). This discrepancy is probably a consequence of the high protein concentration used in the scattering experiments.

There is some discrepancy in slope between the calculated carp parvalbumin scattering curve and our rabbit parvalbumin data near the smallest angles we measured (see Fig. 3 *b*). This may be the result of interparticle scattering effects (20) due to the high protein concentration used in the scattering experiments. This discrepancy corresponds to a smaller radius of gyration, $R_g = 11.8$ Å, for the rabbit parvalbumin when exrapolated to zero angle, but not to zero concentration. It will be important to verify whether this is indeed a concentration effect or whether there are measurable differences between the crystal structure for carp parvalbumin and the terbium-labeled carp and rabbit parvalbumins in solution.

Future improvements in our experimental system, notably in the signal-to-noise ratio of the flux measurements and in the fluorescence cancellation, should also allow us to measure the ~1%-level terbium-terbium term. That would enable us to measure the third side of the triangle with vertices at the center of mass and the two calcium binding sites, in addition to the two sides reported here. This kind of information can be used as a measure of very specific changes in protein conformation, in a way that is not possible with conventional small-angle scattering.

CONCLUDING REMARKS

Our preliminary results using terbium anomalous scattering to measure structural features of parvalbumin demonstrate the utility of the anomalous scattering technique, particularly for calcium binding proteins. The importance of calcium in cellular function and the role parvalbumin and other small calcium binding proteins play in translating free calcium levels into changes in cellular processes make the acquisition of specific structural data essential for understanding the details of this important form of regulation. The study of a variety of questions will be facilitated by the ease with which these proteins are labeled with terbium, and by the ability to derive structural information from these proteins in solution.

Future applications of anomalous scattering include, most directly, other calcium binding proteins (19) labeled with terbium, where important structural questions remain open. The development of more generally applicable labeling techniques, linking terbium and other good anomalous scattering labels to specific structural domains, will expand the range of problems that can be explored with anomalous small-angle solution scattering.

We gratefully acknowlege useful discussions and experimental support from Drs. R. H. Fairclough and J. Reidler.

This work was supported by National Institutes of Health Grant GM 25217. The x-ray scattering experiments were performed at the Stanford

Synchrotron Radiation Laboratory, which is supported by the National Science Foundation under contract DMR 77-27489 and by the National Institutes of Health through Biotechnology Resource Grant RR 01209 in cooperation with the Stanford Linear Accelerator Center and the U.S. Department of Energy.

Received for publication 5 October 1982 and in final form 22 November 1982.

REFERENCES

1. Kratky, O., and I. Pilz. 1978. A comparison of x-ray small angle scattering results to crystal structure analysis and other physical techniques in the field of biological macromolecules. *Q. Rev. Biophys.* 11:39–70.
2. Lye, R. C., J. C. Phillips, D. Kaplan, S. Doniach, and K. O. Hodgson. 1980. White lines in L-edge x-ray absorption spectra and their implications for anomalous diffraction studies of biological materials. *Proc. Natl. Acad. Sci. U. S. A.* 77:5884–5888.
3. Stuhrmann, H. B. 1980. Anomalous dispersion of small-angle scattering of horse-spleen ferritin at the iron K absorption edge. *Acta Crystallogr. Sect. A. Cryst. Phys. Difr. Theor. Gen. Crystallogr.* 36:996–1001.
4. Stuhrmann, H. B., and H. Notbohm. 1981. Configuration of the four iron atoms in dissolved human hemoglobin as studied by anomalous dispersion. *Proc. Natl. Acad. Sci. U. S. A.* 78:6216–6220.
5. Brown, M., R. E. Peierls, and E. A. Stern. 1977. White lines in x-ray absorption. *Phys. Rev. B*15:738–744.
6. Horrocks, W. DeW., and D. R. Sudnick. 1981. Lanthanide ion luminescence probes of the structure of biological macromolecules. *Accounts Chem. Res.* 14:384–392.
7. Reuben, J. 1975. Lanthanides as spectroscopic and magnetic resonance probes in biological systems. *Naturwissen.* 62:172–178.
8. Nieboer, E. 1975. The lanthanide ions as structural probes in biological and model systems. *Struct. Bonding.* 22:1–47.
9. Kretsinger, R. H., and C. E. Nockolds. 1973. Carp muscle calcium-binding protein; II. Structure determination and general description. *J. Biol. Chem.* 248:3313–3326.
10. Bernstein, F. C., T. F. Koetzle, G. J. B. Williams, E. F. Meyer, Jr., M. D. Brice, J. R. Rodgers, O. Kennard, T. Simanouchi, and M. Tasumi. 1977. The protein data bank: A computer-based archival file for macromolecular structures. *J. Mol. Biol.* 112:535–542.
11. Pechére, J.-F., J. Demaille, and J.-P. Capony. 1971. Muscular parvalbumins: preparative and analytical methods of general applicability. *Biochim. Biophys. Acta.* 236:391–408.
12. Rhee, M.-J., D. R. Sudnick, V. K. Arkle, and W. DeW. Horrocks, Jr. 1981. Lanthanide ion luminescence Probes. Characterization of metal ion binding sites and intermetal energy transfer distance measurements in calcium-binding proteins. 1. Parvalbumin. *Biochemistry.* 20:3328–3334.
13. Kopp, M. K. 1979. RC-encoding for position-sensitive proportional counters using low-resistance, metal wire anode and active load capacitance. *Rev. Sci. Instrum.* 50:382–383.
14. Borkowski, C. J., and M. K. Kopp. 1968. New type of position-sensitive detectors of ionizing radiation using risetime measurement. *Rev. Sci. Instrum. 39:1515–1522.*
15. Brown, G. S., and S. Doniach. 1982. The principles of x-ray absorption spectroscopy. *In* Synchrotron Radiation Research. H. Winick and S. Doniach, editors. Plenum Publishing Corp., New York. 353–385.
16. James, R. W.. 1948. The Optical Principles of the Diffraction of X-rays. Cornell University Press, Ithaca, NY. 135–192, 458–512.
17. Forouhi, A. R., B. Sleaford, V. Perez-Mendez, D. de Fontaine, and J. Fodor. 1982. Small-angle scattering system with linear position-sensitive detector. *IEEE Trans. Nucl. Sci.* NS-29:275–278.
18. Radeka, V., and R. A. Boie. 1980. Centroid finding method for position-sensitive detectors. *Nucl. Instrum. Methods.* 178:543–554.
19. Kretsinger, R. H. 1980. Structure and evolution of calcium-modulated proteins. *CRC Crit. Rev. Biochem.* 8:119–174.
20. Kratky, O., and I. Pilz. 1972. Recent advances and applications of diffuse x-ray small-angle scattering on biopolymers in dilute solution. *Q. Rev. Biophys.* 5:481–537.